# Extrusion of Feather Keratin

**Justin R. Barone, Walter F. Schmidt, N. T. Gregoire**

*USDA, ARS, ANRI, EQL, Beltsville, Maryland 20705*

Received 17 December 2004; accepted 27 June 2005
DOI 10.1002/app.23501
Published online in Wiley InterScience (www.interscience.wiley.com).

**ABSTRACT:** Keratin obtained from poultry feathers was extruded at 120°C using a combination of glycerol, water, and sodium sulfite as processing aids. Rheological properties were assessed as a function of water, glycerol, and sodium sulfite content as well as extruder die temperature. The lowest viscosity blends at a constant feather keratin concentration of 60 wt % were found at glycerol concentrations that were higher than the water concentration and sodium sulfite concentrations of 3–4 wt % of the feather keratin fraction. For the melt state, higher or lower sodium sulfite concentrations resulted in increased viscosity. In the solid state, it was observed that processing induced orientation increased the tensile properties of the extrudates. Raman spectroscopy and DSC showed that there was a transition from $\alpha$-helix to $\beta$-sheet at sodium sulfite concentrations of less than 4 wt %. At greater sodium sulfite concentration, increased crystallinity was found, because keratin chains could be extended more during processing. © 2006 Wiley Periodicals, Inc.* J Appl Polym Sci 100: 1432–1442, 2006

**Key words:** biopolymers; proteins; extrusion; Raman spectroscopy

## INTRODUCTION

Extrusion processing of naturally-derived polymers or biopolymers is a topic of much recent interest. Biopolymers from agricultural sources or from the agricultural waste stream are viewed as a viable alternative to petroleum-based polymers, if suitable processing techniques can be found. The biggest advantage of biopolymers over synthetic polymers is that biopolymers are sustainable and environmental friendly. Most research has focused on the thermal processing of carbohydrate biopolymers such as starch.[1,2] However, products made from starch usually have inferior physical properties to comparable products made from synthetic polymers. Therefore, attempts were made at blending starch with synthetic polymers.[3–8] Recently, research has shifted focus to the other biologically important polymer, protein, which may be more robust than carbohydrates. Proteins from wool and feather keratin,[9–11] gelatin,[12] soybean,[13,14] wheat,[15–17] corn,[18–21] milk,[22] and peanut[23] have been processed into films from solution. Solvent casting is tedious and can only be performed on a small scale. In addition, if the solvents are volatile, this would defeat the purpose of environmental-friendliness. Thermal processing is viewed as the easiest method to make biopolymers a "drop-in" replacement for current synthetic polymers. Researchers have thermally processed proteins from soybean,[24,25] sunflower,[26–28] corn,[19,29,30] fish,[31] milk,[32] wheat,[16,33] and feather keratin.[34] This includes compression-molding, injection-molding, extrusion, and internal batch mixing. If biopolymers from sustainable resources are to be used commercially, the biopolymers have to be processed through preferred processing methods. It becomes imperative to identify biopolymers from sustainable resources that can be easily processed using available technology.

Feather keratin could be one such resource. There are ~5 billion pounds of wet poultry feathers (2.5 billion pounds dry) available as the result of U.S. poultry processing.[35] Currently, the feathers are either processed into a low nutritional value animal feed or land-filled, both of which are a liability to the poultry industry. Keratins are defined by the large amount of the amino acid cysteine compared with other proteins.[36] Cysteine (C) is a sulfur-containing amino acid and can form sulfur–sulfur (*S*-S) cystine bonds with other intra- or intermolecular cysteine molecules. Intermolecular cystine bonds are referred to as "crosslinks." The crosslinks plus other protein structural features, like crystallinity and hydrogen-bonding, give keratin high strength and stiffness.[37] The amount of cysteine varies depending on the keratin source. Wool keratin contains 11–17% cysteine, while feather keratin contains about 7% cysteine.[38,39] The cystine bonds deliver strength and stiffness to the keratin in the solid-state, while the cystine bonds are an impediment to processing in the melt-state. Solu-

*Correspondence to:* J. R. Barone (baronej@ba.ars.usda.gov).
Contract grant sponsor: Tyson Foods, Inc.

tion cast cysteine-containing proteins have been prepared using reducing agents to break the cystine bonds.[10] One such reducing agent is sodium sulfite ($Na_2SO_3$), which has been used not only in solution processing of proteins but also in thermal processing as well.[26] Sodium sulfite as a redox reagent is approved for food and drug use and is often used in low quantities as a preservative in food. Therefore, use of small quantities of sodium sulfite would not compromise the environmental-friendliness of a thermally-processed polymer made using it.

In this study, feather keratin waste from poultry processing is blended with sodium sulfite and glycerol and then extruded. The result can be a clear, flexible polymer extrudate if the blend composition and extrusion conditions are right. Glycerol is a commonly used plasticizer in biopolymer processing and can also be obtained from the waste stream of the biodiesel production process or directly from vegetable processing. The effect of feather keratin quality, glycerol concentration, water concentration, sodium sulfite concentration, and extrusion conditions on rheology and solid-state properties is studied. The goal is to produce an easily processed value-added product from a waste stream that is also completely environmental friendly.

## EXPERIMENTAL

### Feather keratin

Feather keratin was obtained from several sources. Pure keratin feather fiber and a mixed fiber/quill fraction were obtained from Featherfiber® Corp. (Nixa, MO). A mixed fiber/quill fraction was also obtained from Tyson Foods, Inc. (Rogers, AR). The Featherfiber Corp. material was thoroughly washed with ethanol using the process developed and patented by the USDA.[40] The Tyson Foods, Inc. material was washed and ground using the process that does not utilize ethanol.[41] Difficulty in obtaining large, consistent supplies of each material for extrusion resulted in the use of the three different materials. Although quantitative comparisons were difficult between each material, qualitative comparisons on blending and extrusion of feather keratin can easily be made.

The as-received feather material was several millimeters in size or larger. Feather material was ground using a Retsch PM 400 ball mill. Feather keratin was loaded into 500 mL stainless steel grinding vessels so that it occupied about a quarter of the volume. The grinding media was four 40-mm stainless steel spheres for a total of 1132 g grinding media. Grinding proceeded at 200 rpm for 10–30 min. The ground feather keratin was then sieved by hand through a sieving stack with sizes ranging from 0.1 to 0.0038 cm. Typical results showing the weight fraction of feather material remaining above each sieve are shown in Figure 1 and grinding of the different feather materials gave similar results. As expected, grinding reduced the average fiber size, from greater than 1 mm for no grinding to 0.589 mm after 10 min, 0.246 mm after 20 min, and 0.0053 mm after 30 min. The properties of feather keratin have been described extensively elsewhere.[34,37,38,42]

### Blend preparation

Sodium sulfite (Mallinckrodt, reagent grade, mol. wt. = 126.04 g/mol, density = 2.63 g/cm$^3$) was dissolved in deionized water (DI-$H_2O$) at various concentrations outlined in the Results and Discussion. Sodium sulfite is a redox reagent and will allow for the breaking of sulfur–sulfur bonds between cysteine residues during extrusion (reduction) resulting in a lower apparent viscosity, $\eta_a$. After extrusion, the sulfur–sulfur bonds can re-form (oxidation). Dissolution of sodium sulfite was aided by stirring. The maximum solubility of sodium sulfite in water is 1 : 3.[43] Glycerol (Sigma–Aldrich, 99+%, mol. wt. = 92.1 g/mol, boiling point = 290°C, density = 1.26 g/cm$^3$) was added to the aqueous solution and further mixed for a few minutes. The ground feather keratin was put into a Waring kitchen blender and the liquid was added. The powder was mixed for 2 min on high-speed, using a plastic spatula to vigorously move material out of the stagnant areas of the blender and into the flow. After 2 min, mixing is stopped, the blender capped and shaken by hand for about a minute, and the high-speed blender mix repeated. During each break in mixing, the mixing blade and blender are felt for heat and the equipment was, at most, warm to touch. The mixing times were decided upon so that liquid would be incorporated into the ground feather keratin without heating the protein.

### Extrusion

Extrusion was performed on a 3/4 in. single-screw extruder (SSE) from Brabender powered by a Prep-Center® drive. The length to diameter ratio of the barrel was 25 : 1 and had a 3 : 1 compression ratio screw. A slit die was used that was $W = 2.54$ cm wide, $H = 0.05$ cm thick, and $L = 0.90$ cm long, and so the aspect ratio of the die is $L/H = 18$. The extruder barrel had three temperature zones and a fourth temperature zone was located on the die, all heated with band heaters. A fifth temperature zone was added at the confluence of the barrel and die and was maintained at the same temperature as the third barrel temperature closest to the die. Extruder motor speed was set and melt pressure, $P$, was measured at the confluence of the barrel to the die, or at the die entrance. Apparent shear stress, $\sigma_a$, was defined as $\sigma_a = PH/2L$. The volumetric flow rate of material, $Q$, was calculated

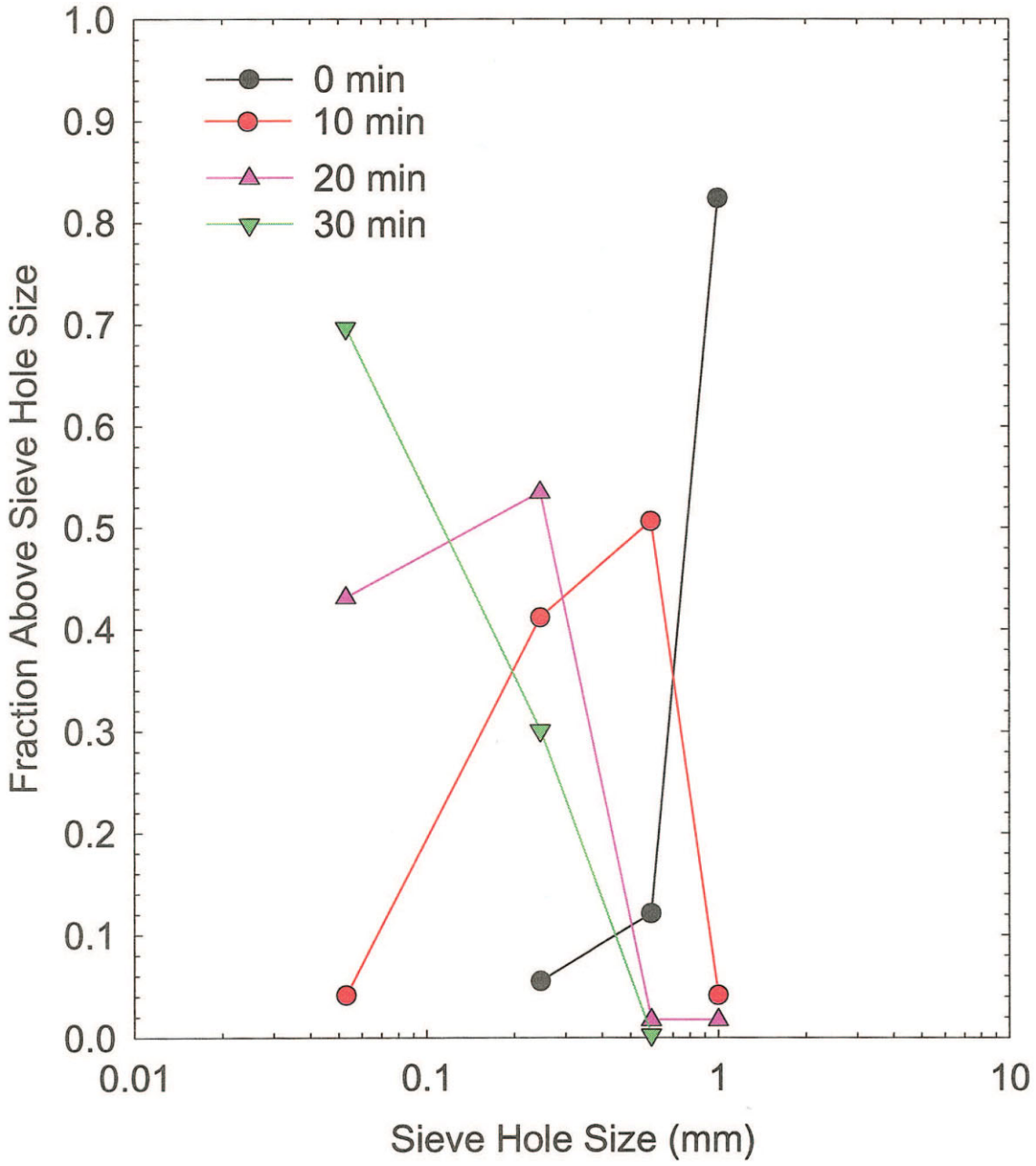


**Figure 1** Feather material size distribution following grinding. [Color figure can be viewed in the online issue, which is available at www.interscience.wiley.com.]

from $Q = m/t$, where $m/\rho t$ was the mass of extrudate flowing per unit time and $\rho$ was the density of the flowing melt. The density of the material was determined from the equation $\rho = (w_k/\rho w_k + w_g/\rho_g + w_w/\rho_w + w_s/\rho_s)^{-1}$, where $w$ is weight fraction, $\rho$ is density, and $k$, $g$, $w$, and $s$ denote keratin, glycerol, water, and sodium sulfite, respectively. Apparent shear rate, $\dot{\gamma}_a$, was then defined as $\dot{\gamma}_a = 6Q/WH^2$. Apparent viscosity, $\eta_a$, was then $\eta_a = \sigma_a/\dot{\gamma}_a$.

### Mechanical testing of extrudates

Mechanical testing of the extrudates was performed immediately after extrusion. Uniaxial tensile testing was performed using a Com-Ten Industries 95 RC Test System. Extrudates 10.2 cm or 15.2 cm long (depending on study) were tested using a gauge length of 5.1 cm or 10.2 cm. The applied crosshead speed was 2.54 cm/min. A minimum of six extrudates for each condition was tested at room temperature and humidity.

### Differential scanning calorimetry

The thermal properties of the extruded feather keratin polymers were assessed using differential scanning calorimetry (DSC). A TA Instruments DSC 910s was

used according to the procedures outlined in ASTM D3417 and D3418. Sample sizes of ~3–5 mg were used in a $N_2$ atmosphere. Only one heating cycle from 30°C to 300°C at 10°C/min was used.

### Raman spectroscopy

A Raman spectrometer from Horiba/Jobin-Yvon was used to examine molecular level interactions of the feather keratin polymer. The instrument was a LabRam HR Raman microscope. The incident beam had a wavelength of 633 nm. The samples were analyzed simply by placing them into the incident beam path under the microscope and recording a spectrum. The spectral range was from 3500 to 200 $cm^{-1}$. The obtained dispersive spectra were baseline corrected and the carbonyl peaks fitted to a Lorentzian equation. The carbonyl peaks were used to compare relative abundance of $\alpha$-helical, $\beta$-sheet, and random coil peptide backbone structures. At least two different sites per sample were scanned as a check for sampling uniformity.

### Solid-state $^{13}$C-NMR

Spectra were collected on a Bruker QE 300 NMR spectrometer at a field strength of 7 T. The $^{13}$C spectra were recorded at 75 MHz with a spectral width of 250 ppm, typically with 1 k scans, 16 k data points, zero-filling to 32 k data points, and a line broadening of 7 Hz. Thin films 2 cm wide were rolled around a 1-mm capillary sealed tube containing DMSO-$d_6$, which was then inserted to fill a standard 5-mm NMR tube. The resulting samples were run deuterium locked as 120°C. The $^{13}$C spectra were collected using an APT pulse program to aid in the potential identification of any unknown peaks (—$CH_2$— and —C═O peaks were all above the baseline, —CH— and —$CH_3$ peaks were always below the baseline).[44]

## RESULTS AND DISCUSSION

### Effect of initial feather keratin size

Blends of the mixed feather fiber/quill material (Featherfiber Corp.) ground for 0, 10, 20, and 30 min, glycerol, DI-$H_2O$, and $Na_2SO_3$ at 60 : 30 : 8 : 2 wt %, respectively, were extruded at a motor speed of 25 rpm. The extruder temperature profile was 100–100–100°C with 120°C at the die. There did not appear to be a significant effect of initial size on the rheological properties. However, Figure 2 shows that the solid-state properties of the extrudates were affected by the initial feather keratin material size. The modulus, $E$, was not affected significantly. But, stress at break, $\sigma_b$, and strain at break, $\varepsilon_b$, decreased as initial material size increased. The creation of the feather keratin polymer in the extruder relies on the reaction of the aqueous sodium sulfite/glycerol with the solid keratin particles. In this case, smaller particles have increased surface area, which allows for more diffusion of the liquid into the solid and a more complete reaction. More completely reacted keratin particles result in better physical properties of the polymer.

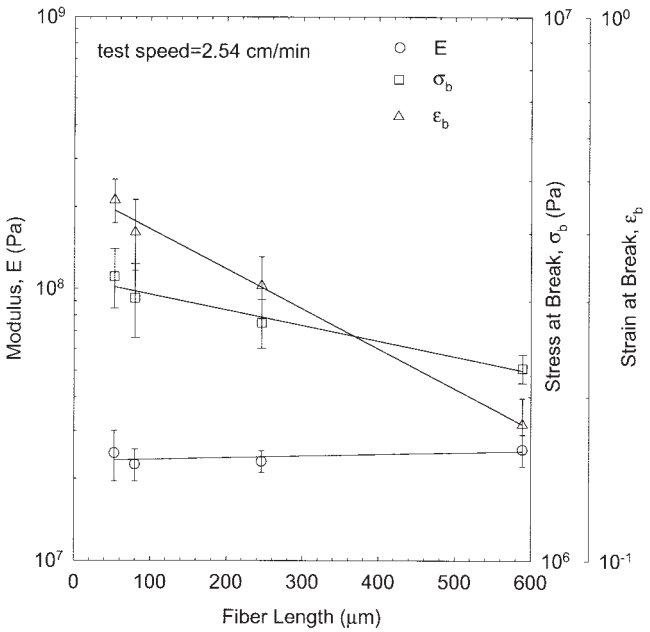


**Figure 2** Effect of initial feather material size on extrudate properties.

### Effect of barrel and die temperature

Figure 3 shows the effect of different barrel and die temperatures on rheology for a mixture of ground feather fiber (Featherfiber Corp.), glycerol, DI-$H_2O$, and $Na_2SO_3$ at 60 : 30 : 8 : 2 wt %, respectively. Two barrel temperature profiles were used over the three barrel heating zones: 100–100–100°C and 120–120–120°C. In addition, two die temperatures of 120 and 140°C were used. The data were the result of several experiments conducted over a range of applied extruder motor speeds. The amount of error between the experiments can be found by comparing the measured apparent viscosity values for a given data set at a constant apparent shear rate. The rheology of feather keratin blends at the specified temperatures shows strong shear-thinning behavior usually displayed by thermoplastic melts, that is, $(\log h_a) \sim (\log \dot{\gamma}_a)^{-0.75}$

In general, lower barrel and die temperature result in higher viscosity. However, there was a more marked lowering of apparent viscosity by using a higher barrel temperature rather than just a higher die temperature. Removal of the die showed that the keratin mixture formed a polymer inside of the extruder

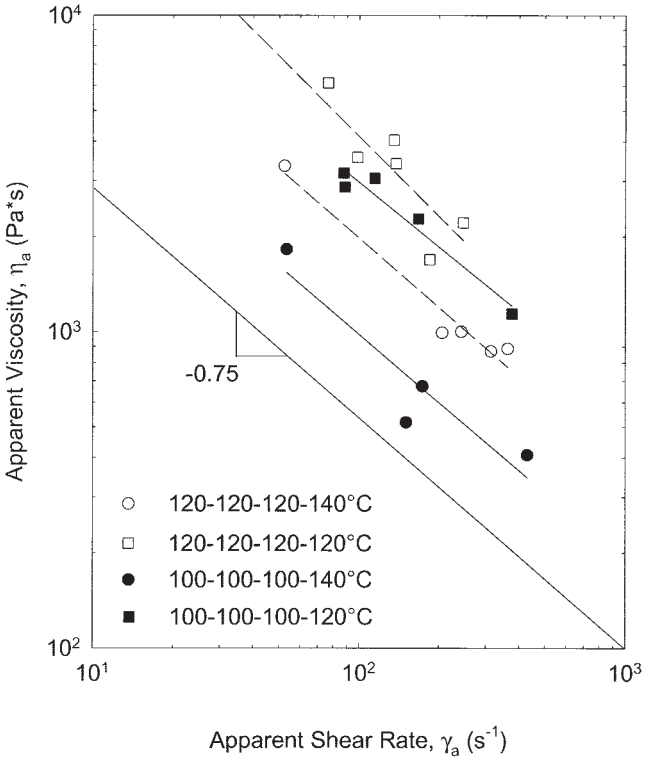


**Figure 3** Rheology of 60 : 30 : 8 : 2 keratin:glycerol:$H_2O$:$Na_2SO_3$ blends at two different barrel and die temperatures.

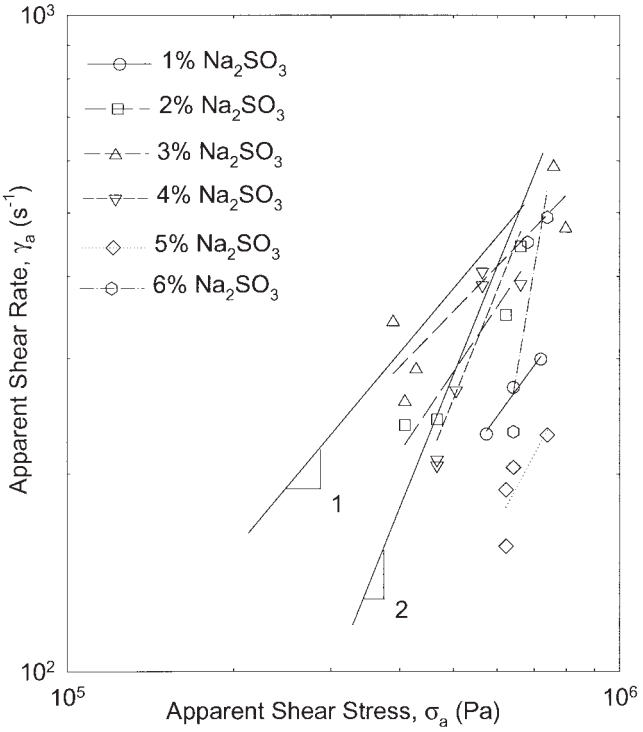


**Figure 5** Rheology of keratin blends with 60% keratin, 20% glycerol, and varying amounts of $Na_2SO_3$ and $H_2O$.

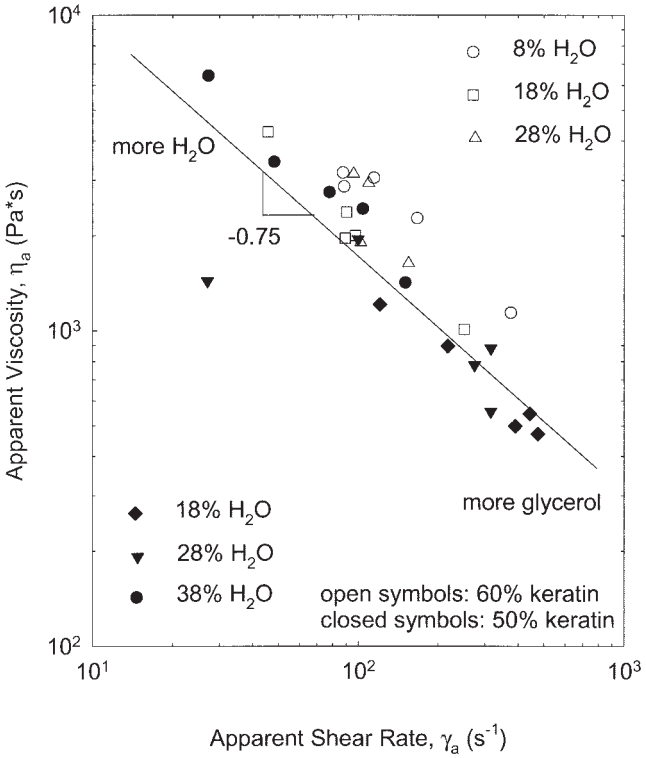


**Figure 4** Rheology of keratin blends with 2% $Na_2SO_3$ and various amounts of keratin, glycerol, and $H_2O$.

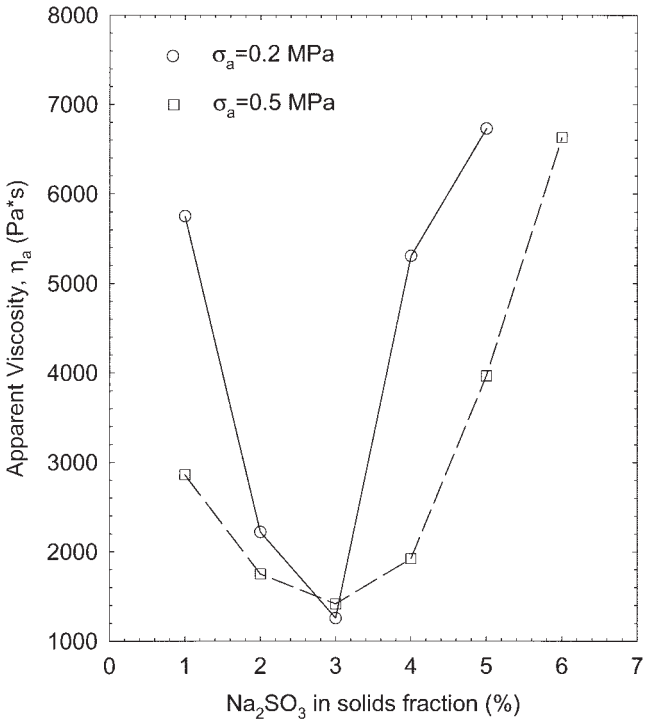


**Figure 6** The effect of $Na_2SO_3$ concentration on apparent viscosity.

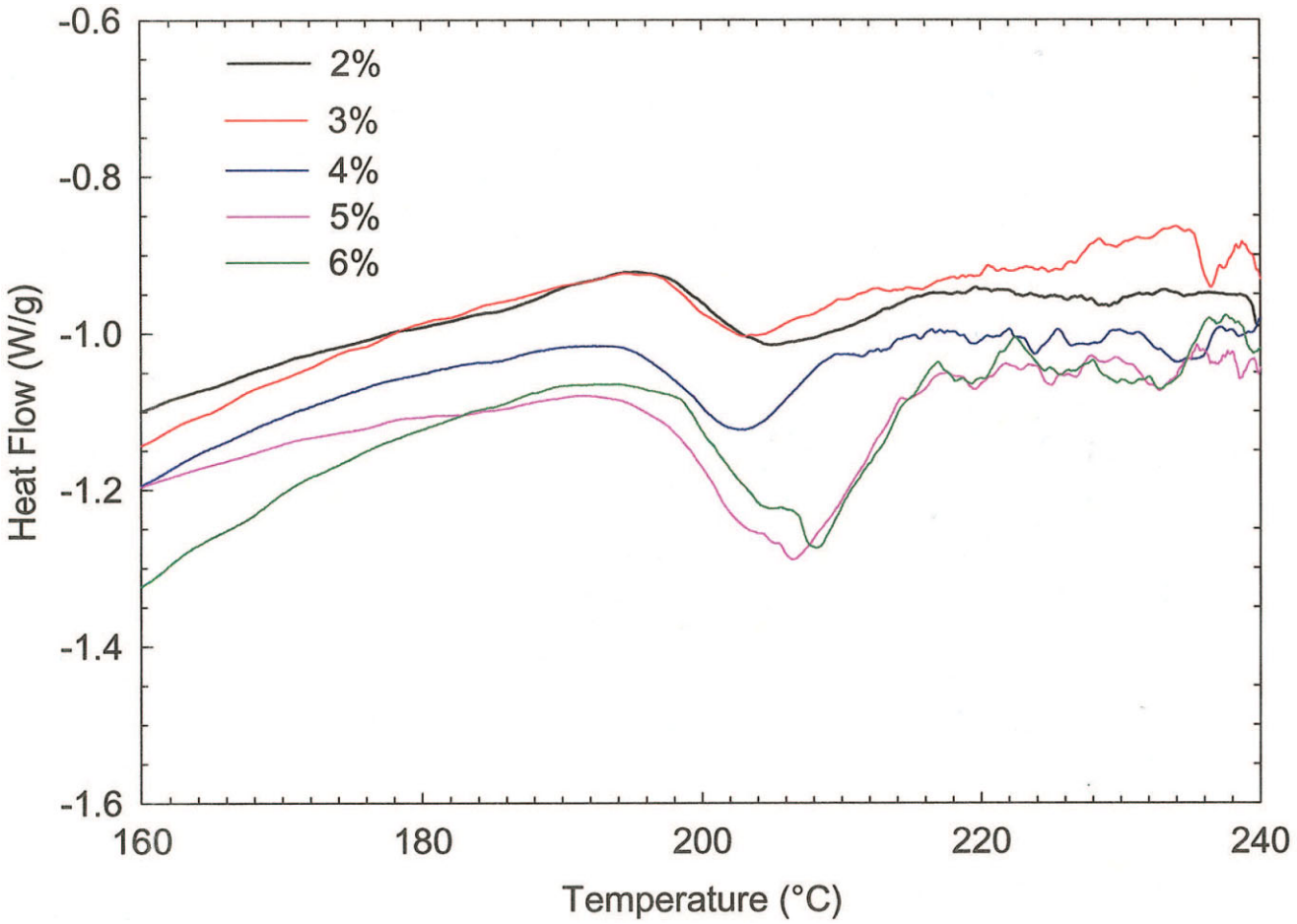


**Figure 7** DSC of blends shown in Figures 5 and 6. [Color figure can be viewed in the online issue, which is available at www.interscience.wiley.com.]

at a barrel temperature of 120°C. However, at a barrel temperature of 100°C, the material exited the extruder the same way it entered, as a powdery mixture. Therefore, the polymer formed inside of the die that was set at 120°C. This was the origin of the larger split between the different barrel temperatures and different die temperatures.

### Effect of water and glycerol content

Figure 4 shows the results of varying the ratio of glycerol to water in a mixture of ground feather fiber keratin (Featherfiber Corp.), glycerol, DI-$H_2O$, and $Na_2SO_3$. The sodium sulfite concentration was held constant at 2 wt % of the total blend concentration, and the feather keratin concentration was either 50 or 60 wt % of the total blend concentration. The balance was a combination of water and glycerol to yield blends of keratin : glycerol : DI-$H_2O$ : $Na_2SO_3$ of 60 : 30 : 8 : 2, 60 : 20 : 18 : 2, 60 : 10 : 28 : 2, 50 : 30 : 18 : 2, 50 : 20 : 28 : 2, and 50 : 10 : 28 : 2 wt %, respectively. The extruder temperature profile was 100–100–100–120°C. The results in Figure 4 show that varying the water to glycerol ratio creates a "master-curve," where more glycerol results in a lower viscosity and faster flow while more water results in a higher viscosity and slower flow. This was probably the result of the loss of water by evaporation during extrusion. The effect of solids concentration was noteable, as the 60 wt % feather keratin data (open symbols) were higher in apparent viscosity (further left on the curve) than the 50 wt % feather keratin data (closed symbols) because there was more liquid in the 50 wt % feather keratin blend. Again, the feather keratin melts showed strong shear-thinning behavior with a scaling similar to the data in Figure 3.

### Effect of sodium sulfite concentration

Figure 5 shows the flow curves for feather keratin blends when the amount of sodium sulfite in the formulation was varied. The feather material used was the mixed quill/fiber fraction from Featherfiber Corp. The amount of feather material and glycerol were kept constant at 60 wt % and 20 wt %, respectively. The sodium sulfite concentration was varied as a percent-

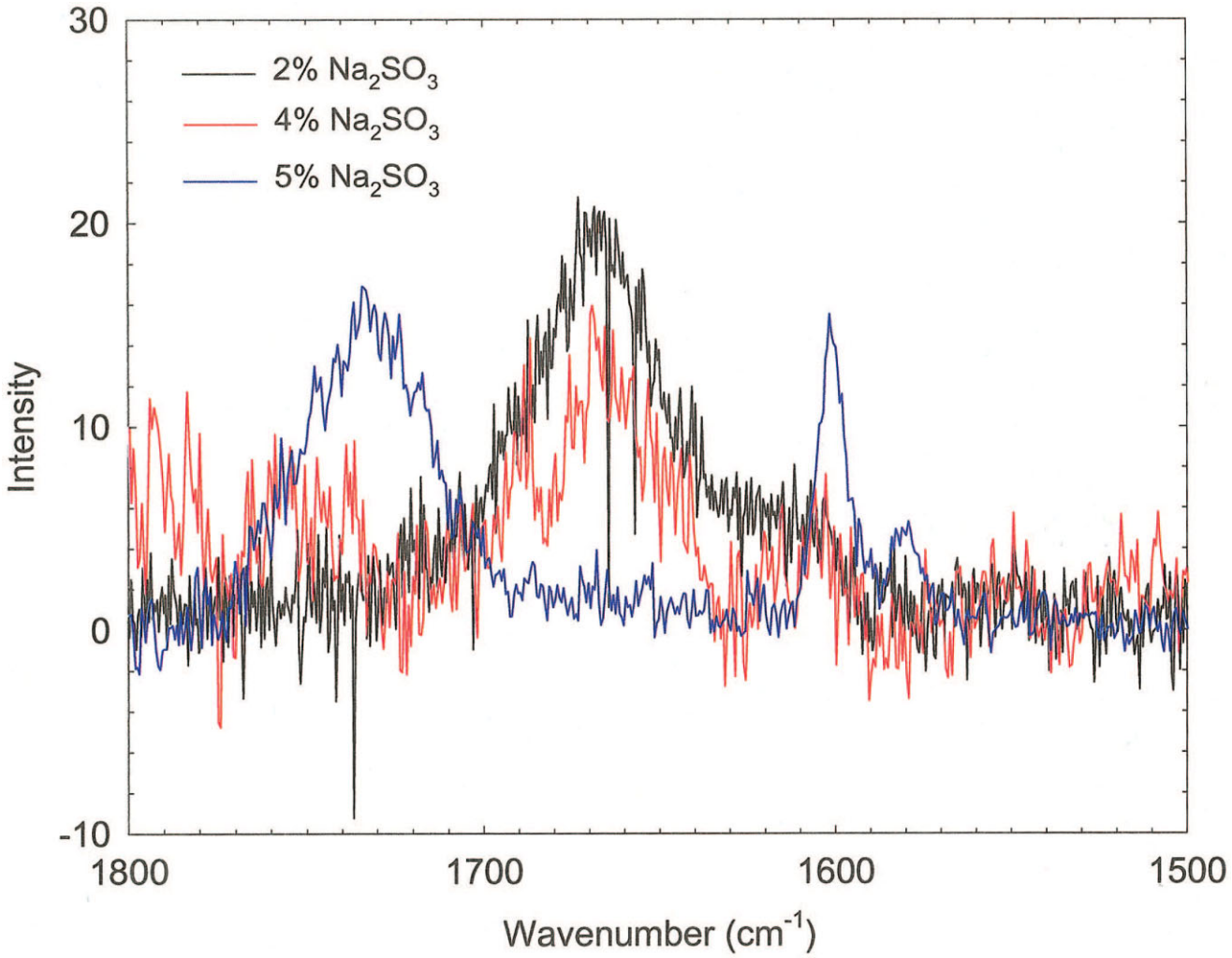


**Figure 8** C═O stretching region of feather keratin obtained with Raman spectroscopy. [Color figure can be viewed in the online issue, which is available at www.interscience.wiley.com.]

age of the feather keratin used. For instance, 1% $Na_2SO_3$ refers to 1% by weight of the 60 wt % of feather keratin used or 0.6 wt % of $Na_2SO_3$ relative to the total formulation. Multiple extruder runs were performed.

The flow curves show that there is a progressive change in the scaling of the apparent shear rate with the apparent shear stress from $(\log \dot{\gamma}_a) \sim (\log \sigma_a)^1$ at 1–3% $Na_2SO_3$ to $(\log \dot{\gamma}_a) \sim (\log \sigma_a)^2$ at 4–6% $Na_2SO_3$. This suggests that there was a change in the molecular structure of the feather keratin polymer with increasing $Na_2SO_3$ concentration. This may indicate that the sodium sulfite was significantly altering the polydispersity or perhaps the amount of branching of the keratin molecules in the melt. Over a similar apparent shear stress range, stronger shear-thinning behavior, that is, increased scaling of the log–log apparent shear rate-apparent shear stress curve, indicates a wider molecular weight distribution or the presence of long chain branches.[45]

The flow curves show that the apparent viscosity progressively decreased as sodium sulfite concentration was increased up to 3% of the feather keratin concentration before increasing again. The apparent viscosity at apparent shear stress values of $\sigma_a$ = 0.2 MPa and 0.5 MPa is plotted as a function of sodium sulfite concentration in Figure 6. A minimum in apparent viscosity is observed in both cases at 3% $Na_2SO_3$ relative to feather keratin or 1.8 wt % of sodium sulfite in the total blend concentration. Orliac et al. observed a decrease of viscosity up to 2.4 wt % sodium sulfite when extruding sunflower protein isolate, followed by a viscosity increase with increased addition of sodium sulfite.[36] These researchers attributed the viscosity increase to an increased breaking of disulfide bonds and perhaps greater protein extension or to the fact that sodium sulfite might act as a charge or complexing agent. Any viscosity reduction because of sodium sulfite would arise from intermolecular *S*-S bond reduction. So the minimum values observed in

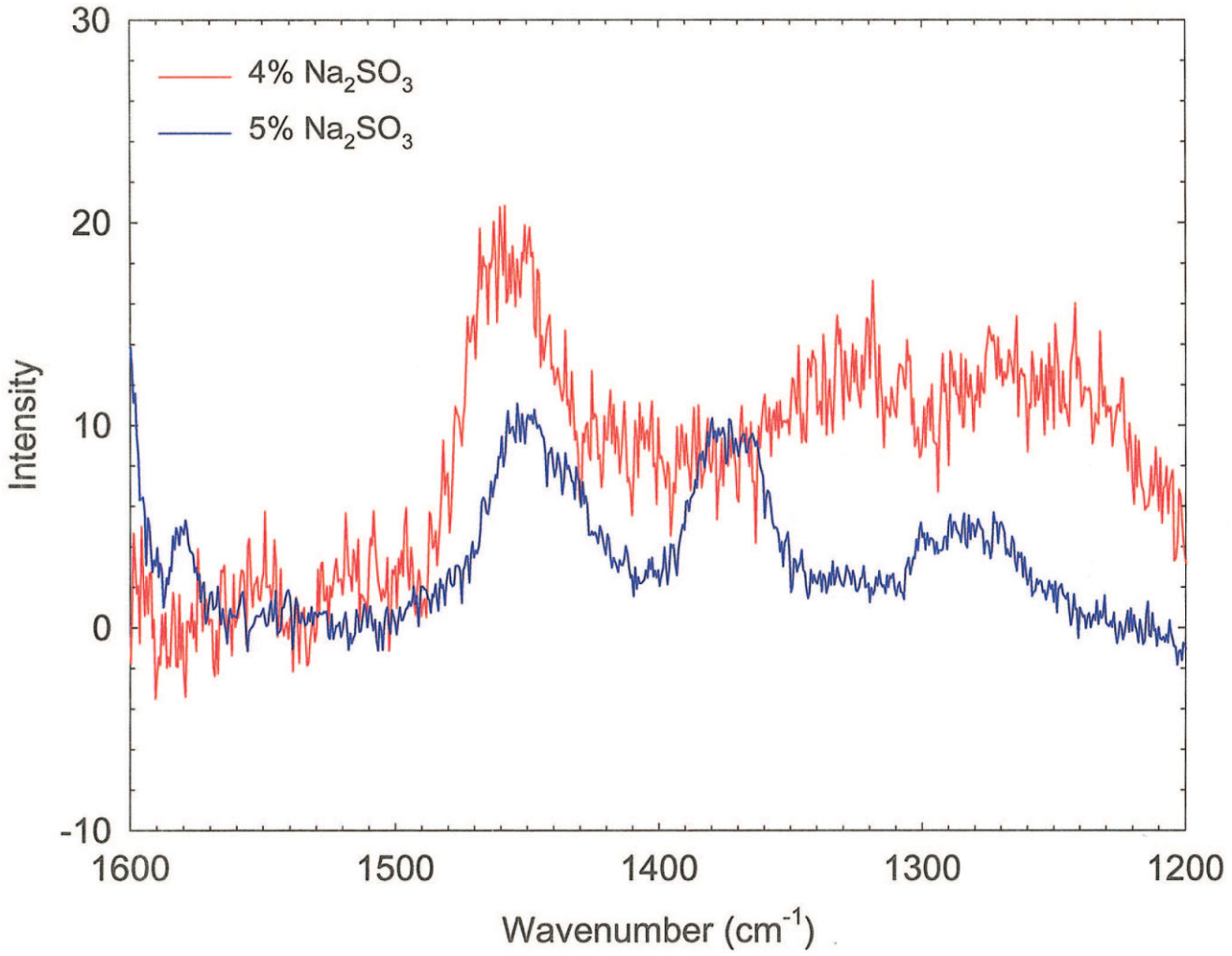


**Figure 9** $CH_2$ region of feather keratin obtained with Raman spectroscopy. [Color figure can be viewed in the online issue, which is available at www.interscience.wiley.com.]

the sodium sulfite concentration studies may reveal the amount of intermolecular disulfide or cystine bonds in the protein. Feather keratin has 7% cysteine in its amino acid sequence.[39] Therefore, about 43% (3/7) of the cysteine amino acids can form intermolecular cystine bonds using this reasoning.

At greater sodium sulfite concentration, the rise in viscosity could at least be partially attributed to the lack of liquid, as evidenced in Figure 2. However, this difference was slight and probably not responsible for such a dramatic change in the rheology. DSC results for the extrudates are plotted in Figure 7 for extrudates obtained at similar extrusion conditions. A crystalline peak is shown for the feather keratin polymers. The crystalline peak becomes more developed with increasing $Na_2SO_3$ concentration. At 5 and 6% $Na_2SO_3$, the peak is large and sharp and at higher temperatures than the 1–4% $Na_2SO_3$ samples. All of the samples were obtained under similar extrusion conditions, and so there does not appear to be any deformation-induced crystallinity from extrusion. However, the notion of Orliac et al. surmising that the keratin molecules become more extended because of less disulfide linkages may be a possible explanation. All of the intermolecular *S*-S bonds may be gone at 3% $Na_2SO_3$, resulting in the lowest melt viscosity. Continued addition of $Na_2SO_3$ may break intramolecular *S*-S bonds, which are holding portions of the keratin molecule together. *S*-S bonds between two different molecules may be more accessible than *S*-S bonds between different portions of the same molecule, resulting in the observed behavior. If there are less intramolecular disulfide linkages, more of the keratin molecule is free to rearrange in the reduced melt state and crystallize upon oxidation, resulting in increased crystallinity.

Raman spectroscopy is one possible method to monitor disulfide linkages in keratin.[46,47] The sulfur–sulfur (*S*-S) bonds appear as weak peaks in the 500–550 $cm^{-1}$ range of the spectrum. In Raman experiments on the feather keratin polymers, no *S*-S peaks

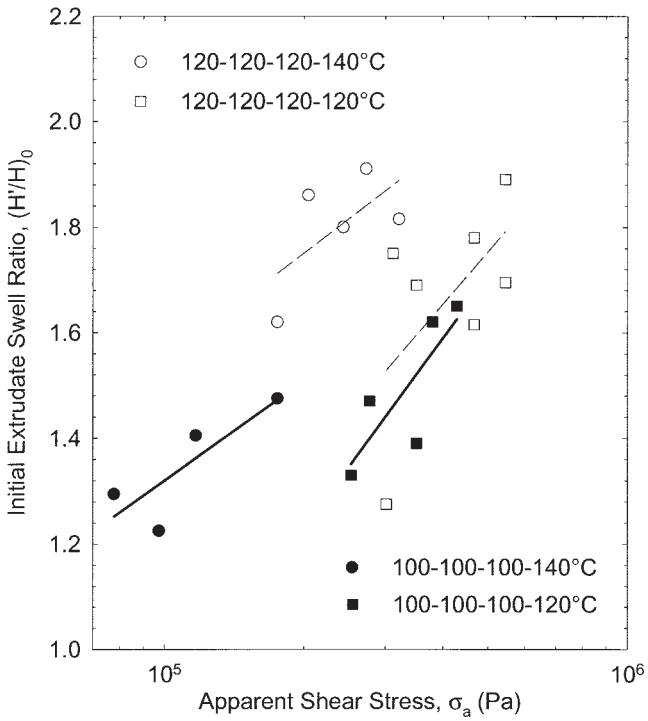


**Figure 10** Initial extrudate swell ratio for rheological data depicted in Figure 3.

were found outside of the background noise of the spectra, probably because they were too weak. However, other discernible peaks reveal important information about the structure of the polymers as a function of sodium sulfite concentration. Figure 8 shows the carbonyl region of the Raman spectrum for the keratin polymers. Shown are the 2, 4, and 5% $Na_2SO_3$ samples. At 2% $Na_2SO_3$, there is a strong peak at 1665 $cm^{-1}$ indicative of a $\beta$-sheet fraction of keratin. There is a small shoulder on this peak at about 1610 $cm^{-1}$, which may be indicative of the carbon–carbon double bond on the aromatic ring of tyrosine or phenylalanine, which comprise 1.4 and 3.1 wt % of feather keratin, respectively.[46] As $Na_2SO_3$ concentration is increased to 4%, the peak at 1665 $cm^{-1}$ decreases while the peak at 1610 $cm^{-1}$ becomes more pronounced. At 5% $Na_2SO_3$, the amide carbonyl peak at 1665 $cm^{-1}$ completely disappears, with two pronounced peaks at 1605 and 1580 $cm^{-1}$ appearing. The peaks at 1605 and 1580 $cm^{-1}$ have been assigned to tyrosine and phenylalanine, respectively.[46] These changes together demonstrate that a major disruption of the $\beta$-sheet formation occurred. As $Na_2SO_3$ concentration was increased, more disulfide bonds were reduced and more of the keratin molecule was exposed to additional redox reaction. In this case, there was a significant rearrangement of the keratin molecule to expose the portions that contain aromatic rings. This was not so surprising as the portions of the peptide backbone with the large aromatic side chains may be too sterically hindered to return to their original position once the cystine bonds holding them in a strained location were broken. The appearance of a new peak at 1735 $cm^{-1}$ for the 5% $Na_2SO_3$ extrudate may be indicative of degradation or rearrangements along the peptide backbone. These changes at some sites in keratin could potentially disrupt the uniformity of the $\beta$-sheet as a whole.

Additional evidence of the rearrangement of the keratin backbone after redox treatment is found in Figure 9. The 4% and 5% $Na_2SO_3$ spectra are shown, which was where the transition from low to high crystallinity was detected in DSC. The $CH_2$ scissor peak in the 4% spectrum at 1460 $cm^{-1}$ was observed at 1450 $cm^{-1}$ in the 5% spectrum. The appearance of a new peak at 1375 $cm^{-1}$ in the 5% spectrum is at the normal frequency for symmetrical $CH_3$ scissors motion, for example, on alanine.[48] In the absence of the $\beta$-sheet in the 5% sample, the mobility of one or more of the —$CH_3$ groups on keratin may have increased. All of this is consistent with previous results where Nishikawa et al. show that reduction and subsequent oxidation of human hair keratin results in the decrease of the $\alpha$-helix conformation with new disordered structures forming.[49]

## Extrudate swell

The extrudate swell ratio is defined as the extrudate thickness, $H'$, relative to the slit die thickness, $H$. In

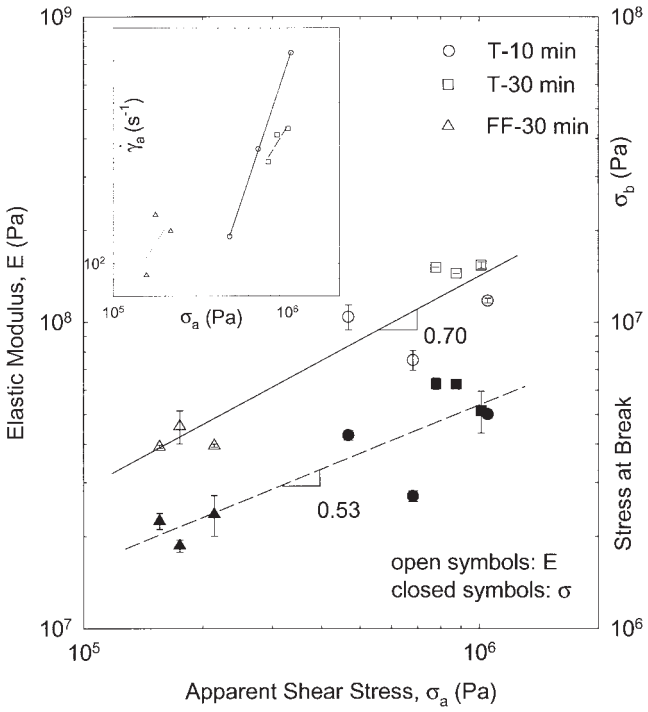


**Figure 11** Effect of initial material quality on extrudate physical properties.

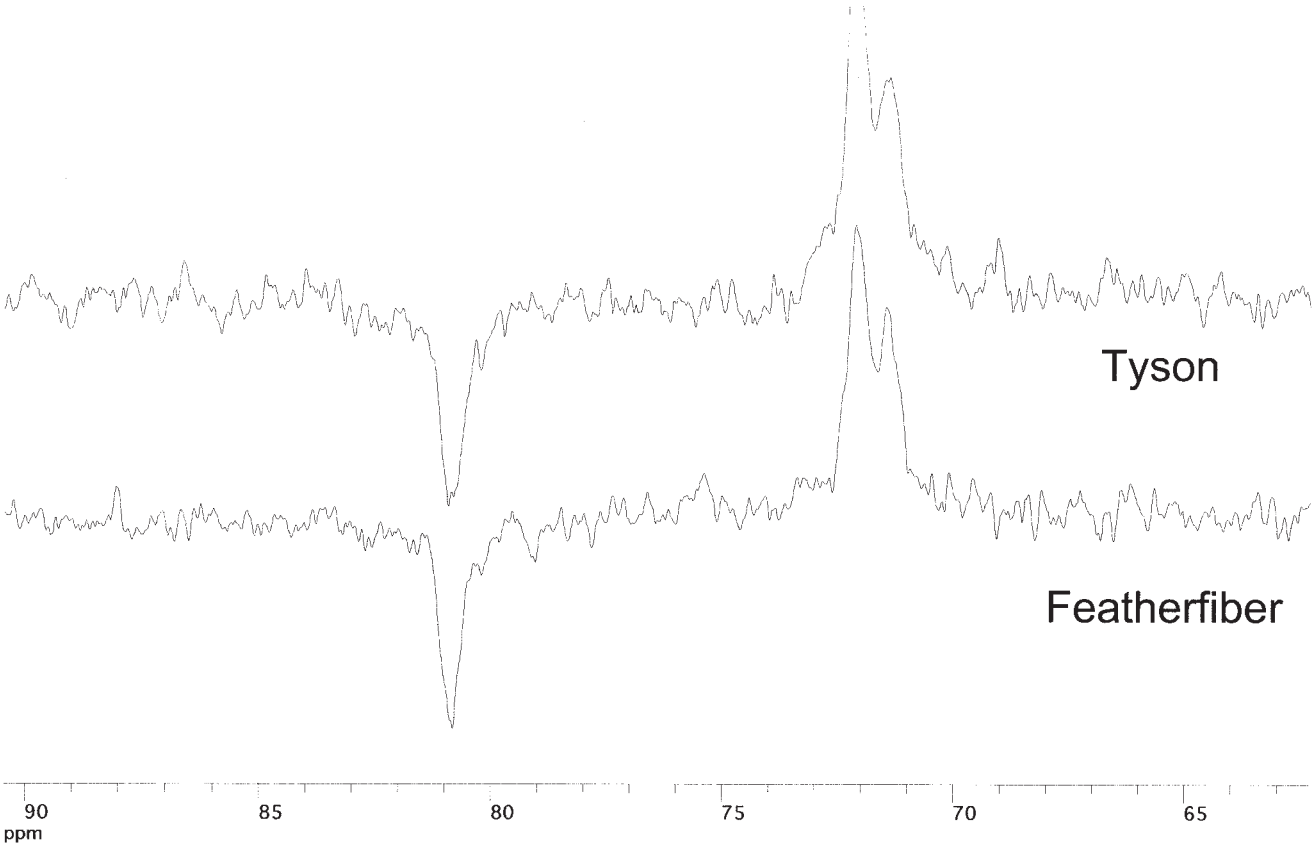


**Figure 12** Solid-state NMR spectra of Tyson and Featherfiber extrudates.

this study, the initial extrudate swell ratio, $(H'/H)_0$ is plotted, which is the swell ratio immediately upon exiting the die.[50,51] Extrudate swell is the recovery of deformation imposed onto the flowing polymer during extrusion. Figure 10 shows the initial extrudate swell ratio for the rheological data presented in Figure 3. The extrudate swell grew with increasing apparent shear stress, which was expected because the higher the apparent shear stress, the more imposed deformation. At a given apparent shear stress, higher die temperatures result in more extrudate swell. Extrudate swelling of 20–80% was observed for the blends over the range of apparent shear stress used. Large amounts of extrudate swell are not uncommon for polymers and are important in some applications like film extrusion or blowing, where the polymeric film exits the die and then is drawn-down a large amount by a calender or film blower. Large amounts of extrudate swell correlate with melt elasticity or large first normal stress difference, $N_1$.[52] So, the feather keratin polymer has a fair amount of melt elasticity that would make it preferential to use in film making processes. Film made from feather keratin would be biodegradable and could therefore be used for packaging, for instance.

**Quality of feather keratin material**

Figure 11 shows the solid-state tensile properties of three different extrudates plotted as a function of apparent shear stress during extrusion. The three different extrudates were the material from Tyson Foods, Inc. ground for 10 (T-10 min) and 30 (T-30 min) min and the feather fiber fraction from Featherfiber Corp. ground for 30 (FF-30 min) min. All blends were 60 : 30 : 8 : 2 wt % of feather keratin, glycerol, DI-$H_2O$, and $Na_2SO_3$, respectively. Extrusion occurred at a temperature profile of 100–100–100–120°C. Shown in the inset is the rheological data corresponding to the tensile data. Both the modulus and breaking strength of the extrudates increased with the increasing apparent shear stress, during extrusion. It is well known that polymer molecules are more oriented at higher extrusion stresses and increased molecular orientation was a factor in the higher modulus and breaking stress observed. However, the three different feather keratin samples also contributed to the observed rheological and mechanical differences.

The difference in properties between identical blends of samples T-10 min, T-30 min, and FF-30 min originated in how effective the glycerol was in plasticizing each sample. Nuclear magnetic resonance

(NMR) spectroscopy of the extrudates showed sharper peaks at 81 ppm and 72 ppm for the Featherfiber keratin material over the Tyson keratin material (Fig. 12). The difference in the peak quality was indicative of increased hydrogen bonding in the Tyson keratin material, which may also be responsible for the increased mechanical properties. New peaks at 73 ppm and 69 ppm for the Tyson keratin material indicate the presence of a lipid contaminant, which was not eradicated during cleaning. The increased hydrogen bonding in the Tyson material was not surprising, because it was not cleaned and dried as thoroughly as the Featherfiber material and therefore contains more water. In addition, less glycerol was probably available for keratin plasticization because some associated with the lipid. In contrast, all of the glycerol used in the Featherfiber material went to keratin plasticization as seen by the sharp peaks at 81 and 72 ppm. So, the FF-30 min extrudate was more plasticized, which resulted in a lower melt viscosity, a more flexible material, and a lower strength to break. Coincidentally, the T-30 min material, with a smaller particle size, still showed increased physical properties over the T-10 min sample, with a larger particle size, concurrent with Figure 2.

The authors thank Horiba/J. Yvon for the use of their LabRam HR Raman microscope.

## References


1. Rouilly, A.; Rigal, L. J Macromol Sci Polym Rev 2002, C42, 441.
2. Bayer, R. K.; Lindemann, S.; Dunkel, M.; Cagiao, M. E.; Ania, F. J Macromol Sci Phys 2001, B40, 733.
3. DeGraaf, R. A.; Janssen, L. P. B. M. Polym Eng Sci 2001, 41, 584.
4. Biresaw, G.; Carriere, C. J. J Polym Sci Polym Phys 2001, 39, 920.
5. Park, J. W.; Im, S. S.; Kim, S. H.; Kim, Y. H. Polym Eng Sci 2000, 40, 2539.
6. Zhou, G.; Willett, J. L.; Carriere, C. J. Polym Eng Sci 2001, 41, 1365.
7. Averous, L.; Fringant, C. Polym Eng Sci 2001, 41, 727.
8. Rodriguez-Gonzalez, F. J.; Ramsay, B. A.; Favis, B. D. Polymer 2003, 44, 1517.
9. Yamauchi, K.; Yamauchi, A.; Kusunoki, T.; Kohda, A.; Konishi, Y. J Biomed Mater Res 1996, 31, 439.
10. Schrooyen, P. M. M.; Dijkstra, P. J.; Oberthur, R. C.; Bantjes, A.; Feijen, J. J Agric Food Chem 2000, 48, 4326.
11. Schrooyen, P. M. M.; Dijkstra, P. J.; Oberthur, R. C.; Bantjes, A.; Feijen, J. J Agric Food Chem 2001, 49, 221.
12. Bigi, A.; Borghi, M.; Cojazzi, G.; Fichera, A. M.; Panzavolta, S.; Roveri, N. J Therm Anal Cal 2000, 61, 451.
13. Okamoto, S.; Setagaya-ku, T. Cereal Food World 1978, 23, 256.
14. Kim, K. M.; Marx, D. B.; Weller, C. L.; Hanna, M. A. J Am Oil Chem Soc 2003, 80, 71.
15. Mangavel, C.; Barbot, J.; Gueguen, J.; Popineau, Y. J Agric Food Chem 2003, 51, 1447.
16. Domenek, S.; Feuilloley, P.; Gratraud, J.; Morel, M.-H.; Guilbert, S. Chemosphere 2004, 54, 551.
17. Irissin-Mangata, J.; Baudin, G.; Boutevin, B.; Gontard, N. Eur Polym J 2001, 37, 1533.
18. Yoshino, T.; Isobe, S.; Maekawa, T. J Am Oil Chem Soc 2002, 79, 345.
19. Wang, Y.; Rakotonirainy, A. M.; Padua, G. W. Starch 2003, 55, 25.
20. Tillekeratne, M.; Easteal, A. J. Polym Int 2000, 49, 127.
21. Wei, W.; Baianu, I. C. Macromol Symp 1999, 140, 197.
22. McHugh, T. H.; Aujard, J.-F.; Krochta, J. M. J Food Sci 1994, 59, 416.
23. Liu, C.-C.; Tellez-Garay, A. M.; Castell-Perez, M. E. Lebensm-Wiss u-Technol 2004, 37, 731.
24. Vaz, C. M.; Mano, J. F.; Fossen, M.; van Tuil, R. F.; de Graaf, L. A.; Reis, R. L.; Cunha, A. M. J Macromol Sci Phys 2002, B41, 33.
25. Liang, F.; Wang, Y.; Sun, X. S. J Polym Eng 1999, 19, 383.
26. Orliac, O.; Silvestre, F.; Rouilly, A.; Rigal, L. Ind Eng Chem Res 2003, 42, 1674.
27. Orliac, O.; Silvestre, F. Macromol Symp 2003, 197, 193.
28. Orliac, O.; Rouilly, A.; Silvestre, F.; Rigal, L. Ind Crops Prod 2003, 18, 91.
29. di Gioia, L.; Guilbert, S. J Agric Food Chem 1999, 47, 1254.
30. di Gioia, L.; Cuq, R.; Guilbert, S. Macromol Symp 1999, 144, 365.
31. Cuq, B.; Gontard, N.; Guilbert, S. Lebensm-Wiss u-Technol 1999, 32, 107.
32. Sothornvit, R.; Olsen, C. W.; McHugh, T. H.; Krochta, J. M. J Food Sci 2003, 68, 1985.
33. Pommet, M.; Redl, A.; Morel, M.-H.; Domenek, S.; Guilbert, S. Macromol Symp 2003, 197, 207.
34. Barone, J. R.; Schmidt, W. F.; Liebner, C. F. E. J Appl Polym Sci, to appear.
35. Parkinson, G. Chem Eng 1998, 105, 21.
36. Vincent, J. Structural Biomaterials; Princeton University Press: New Jersey, 1990.
37. Fraser, R. D. B.; MacRae, T. P. In Symposia of the Society for Experimental Biology Number XXXIV; Vincent, J. F.V.; Currey, J. D., Eds.; Cambridge University Press: Cambridge, 1980.
38. Fraser, R. D. B.; MacRae, T. P.; Rogers, G. E.; Keratins: Their Composition, Structure, and Biosynthesis; Charles C. Thomas: Illinois, 1972.
39. Arai, K. M.; Takahashi, R.; Yokote, Y.; Akahane, K. Eur J Biochem 1983, 132, 501.
40. Gassner, G.; Schmidt, W.; Line, M. J.; Thomas, C.; Water, R. M. U.S. Pat. 5,705,030 (1998).
41. Griffith, B. A. U.S. Pat. Appl. 2002/0079074 A1 (2002).
42. Schmidt, W. F.; Jayasundera, S. In Natural Fibers Plastics, and Composites-Recent Advances; Wallenberger, F.; Weston, N., Eds.; Kluwer Academic: Massachusetts, 2003.
43. Windholz, M.; Budavari, S.; Blumetti, R. F.; Otterbein, E. S. The Merck Index, 10th ed.; Merck and Company: Rahway, NJ, 1983.
44. Braun, S.; Kalinowski, H.-O.; Berger, S. 150 and More Basic NMR Experiments; Wiley-VCH: Weinheim, 1998.
45. Macosko, C. Rheology: Principles Measurements, and Applications; VCH Publishers: New York, 1994.
46. Akhtar, W.; Edwards, H. G. M. Spectrochim Acta A 1997, 53, 81.
47. Edwards, H. G. M.; Hunt, D. E.; Sibley, M. G. Spectrochim Acta A 1998, 54, 745.
48. Alpert, N. L.; Keiser, W. E.; Szymanski, H. A. IR-Theory and Practice of Infrared Spectroscopy; Plenum/Rosetta: New York, 1970.
49. Nishikawa, N.; Tanizawa, Y.; Tanaka, S.; Horiguchi, Y.; Asakura, T. Polymer 1998, 39, 3835.
50. Yang, X.; Wang, S.-Q.; Chai, C. J Rheol 1998, 42, 1075.
51. Koopmans, R. J. Polym Eng Sci 1992, 32, 1750.
52. Tanner, R. I. J Polym Sci Polym Phys 1970, 8, 2067.